Environ. Eng. Res. 2014; 19(3): 247-253
http://dx.doi.org/10.4491/eer.2014.029

pISSN 1226-1025
eISSN 2005-968X

Characterization of Quintinite Particles in Fluoride Removal from Aqueous Solutions

Jae-Hyun Kim, Jeong-Ann Park, Jin-Kyu Kang, Jeong-Woo Son, In-Geol Yi, Song-Bae Kim†

Environmental Functional Materials & Biocolloids Laboratory, Seoul National University, Seoul 151-921, Korea

ABSTRACT

The aim of this study was to characterize quintinite in fluoride removal from aqueous solutions, using batch experiments. Experimental results showed that the maximum adsorption capacity of fluoride to quintinite was 7.71 mg/g. The adsorption of fluoride to quintinite was not changed at pH 5–9, but decreased considerably in highly acidic (pH < 3) and alkaline (pH > 11) solution conditions. Kinetic model analysis showed that among the three models (pseudo-first-order, pseudo-second-order, and Elovich), the pseudo-second-order model was the most suitable for describing the kinetic data. From the nonlinear regression analysis, the pseudo-second-order parameter values were determined to be q_e=0.18 mg/g and k_2=28.80 g/mg/hr. Equilibrium isotherm model analysis demonstrated that among the three models (Langmuir, Freundlich, and Redlich-Peterson), both the Freundlich and Redlich-Peterson models were suitable for describing the equilibrium data. The model analysis superimposed the Redlich-Peterson model fit on the Freundlich fit. The Freundlich model parameter values were determined from the nonlinear regression to be K_F=0.20 L/g and $1/n$=0.51. This study demonstrated that quintinite could be used as an adsorbent for the removal of fluoride from aqueous solutions.

Keywords: Adsorption, Batch experiment, Fluoride, Hydrotalcite-like particles, Quintinite

1. Introduction

Quintinite is a carbonate mineral with a hexagonal crystal system. It has the chemical formula of $Mg_4Al_2(OH)_{12}CO_3 \cdot 3H_2O$, which is included in the family of hydrotalcite-like (HTL) particles [1]. Hydrotalcite is a carbonate mineral that is rare in nature, with the general formula of $Mg_6Al_2(CO_3)(OH)_{16}{\cdot}4(H_2O)$. Hydrotalcite mineral is a layered double hydroxide (LDH), with carbonate anions lying between the structural layers [2]. The HTL particles are similar to hydrotalcite mineral, which can be easily synthesized in the laboratory. They have the general formula of $[M(II)_{1-x}M(III)_x(OH)_2]^{x+}[A^{n-}x/n]^{x-} \cdot mH_2O$, where M(II) is the divalent cation (Mg, Ni, Zn, Co, Mn, etc.), M(III) is the trivalent cation (Al, Fe, Cr, V, etc.), A^{n-} is the interlayer anion (Cl^-, NO_3^-, CO_3^{2-}, SO_4^{2-}, etc.) of valence n, and x is the molar ratio of M(III)/[M(II)+M(III)]. They consist of positively charged brucite $[Mg(OH)_2]$-like layers $[M(II)_{1-x}M(III)_x(OH)_2]^{x+}$ and negatively-charged interlayers $[A^{n-}_{x/n}]^{x-} \cdot mH_2O$. They are a class of anionic clays with high surface area and large anion exchange capacity [3, 4]. The HTL particles have been used as adsorbents for the removal of oxyanions, including chromate, phosphate, nitrate, borate, arsenate/arsenite, and selenite/selenite [5].

Fluoride is an essential micronutrient for human health that prevents dental caries, and helps dental enamel calcification. However, at concentrations greater than 1.5 mg/L, fluoride can cause dental/skeletal fluorosis and neurological damage [6]. The contamination of fluoride in drinking water resources is a serious environmental problem worldwide. Fluoride contamination in surface and ground water can come from natural geological sources (fluorite, biotites, granite, basalt, etc.), and from industrial wastewater (semiconductor manufacturing, electroplating, glass and ceramic production, etc.) [7]. In many countries, fluoride occurs naturally in groundwater at concentrations exceeding the guidelines of the World Health Organization (1.5 mg/L), causing serious health problems [8]. Adsorption is widely used for fluoride removal from aqueous solutions, due to its cost effectiveness and simplicity of operation. Various adsorbents have been applied for fluoride removal, including activated alumina, activated carbon, granular ferric hydroxide, limestone, fly ash, and clay [9, 10].

Recently, some researchers used Mg/Al, Zn/Al, and Mg/Al/Fe type HTL particles for fluoride removal [6, 11]. Batistella et al. [12] evaluated the effect of acid activation on the removal of fluoride by Mg/Al type particles. Mandal and Mayadevi [13] performed kinetic, equilibrium, and thermodynamic studies for fluoride removal by Zn/Al type particles. Others used mixed metal oxides (MMO) derived from the various HTL particles, via calcination

Received May 20, 2014 **Accepted** July 3, 2014

† Corresponding author
E-mail: songbkim@snu.ac.kr
Tel: +82-2-880-4587 Fax: +82-2-873-2087

for fluoride removal [14-19]. Cai et al. [7] examined the competitive adsorption of fluoride and phosphate by Mg/Al MMO. Zhou et al. [20] analyzed the characteristics of Li/Al MMO in fluoride adsorption in water. In addition, Mandal and Mayadevi [21] used Zn/Al MMO for fluoride adsorption.

The aim of this study was to characterize quintinite in fluoride removal from aqueous solutions. The characteristics of synthetic quintinite particles were elucidated using transmission electron microscopy (TEM), X-ray diffractometry (XRD), nitrogen gas (N_2) adsorption-desorption experiment, and X-ray photoelectron spectroscopy (XPS). Batch experiments were performed to examine the effect of adsorbent dosage, reaction time, initial fluoride concentration, and initial solution pH on the adsorption of fluoride to quintinite. Kinetic and equilibrium isotherm models were used to analyze the batch experimental data.

2. Materials and Methods

2.1. Synthesis and Characterization of Quintinite Particles

All chemicals used for the experiments were purchased from Sigma-Aldrich. Quintinite particles were prepared by the following procedures. The particles were synthesized by co-precipitating mixtures of magnesium nitrate [$Mg(NO_3)_2 \cdot 6H_2O$] and aluminum nitrate [$Al(NO_3)_3 \cdot 9H_2O$]. A 700 mL solution (Mg/Al molar ratio = 2) of $Mg(NO_3)_2 \cdot 6H_2O$ (1 mol) and $Al(NO_3)_3 \cdot 9H_2O$ (0.5 mol) was added drop-wise, using a peristaltic pump (QG400; Fasco, Springfield, MO, USA), at 3 mL/min, into 1,000 mL of alkali solution (pH = 13) consisting of sodium hydroxide (NaOH) and sodium carbonate (Na_2CO_3), with intensive stirring at room temperature. The resulting precipitates were aged at 65°C for 18 hr in mother liquor. The precipitates were thoroughly washed with deionized water to remove excess sodium, and then final suspensions were centrifuged at 8,500 rpm for 20 min. The washed precipitates were oven-dried again at 65°C for 24 hr, and then pulverized in a ball mill. The pulverized precipitates were passed through US Standard Sieve No. 100 (grain size = 0.149 mm). The particles used for the experiments were finally obtained through oven drying at 105°C.

TEM (JEM-1010; JEOL Ltd., Tokyo, Japan) was used to take images of the particles. The particle size was determined by analysis of the TEM image (number of particle = 71) using ImageJ 1.43u software (National Institutes of Health, Bethesda, MD, USA). The mineralogical and crystalline structural properties were examined using XRD (D8 ADVANCE; Bruker, Germany) with a CuKα radiation of 1.5406 Å, at a scanning speed of 0.6°/sec. N_2 adsorption-desorption experiments were performed using a surface area analyzer (BELSORP-max; BEL Japan Inc., Osaka, Japan), after the sample was pretreated at 120oC. From the N2 adsorption-desorption isotherms, the specific surface area, total pore volume, and mesopore volume were determined by Brunauer-Emmett-Teller (BET) and Barrett-Joyner-Halenda (BJH) analyses. XPS (XPS Sigma Probe; Thermo VG, West Sussex, UK) measurement was performed with monochromatic Al Kα radiation.

2.2. Fluoride Adsorption Experiments

The desired fluoride solution was prepared by diluting the stocking fluoride solution (1,000 mg/L), which was made from sodium fluoride (NaF). The first batch experiments were performed at different dosages of adsorbent (quintinite), ranging from 0.1 to 2.0 g in 30 mL solution. Adsorbent was added to 30 mL of fluoride solution (initial concentration = 10 mg/L), in 50 mL polypropylene conical tubes. The tubes were shaken at 25°C and 100 rpm, using a culture tube rotator (MG-150D; Mega Science, Seoul, Korea). The samples were collected 6 hr after the reaction, and were filtered through a 0.45-μm membrane filter. The fluoride concentration was measured using a fluoride ion selective electrode (9609BNWP; Thermo Scientific, Waltham, MA, USA). For the fluoride measurement, total ionic strength adjustment buffer solution (58 g of NaCl, 57 mL of CH_3COOH, and 150 mL of 6 M NaOH in 1,000 mL of deionized water) was used to prevent the interference of other ions.

Based on the results from the above tests, further batch experiments were conducted, at the adsorbent dose of 1.5 g in 30 mL solution. The second batch experiments were performed at the initial fluoride concentrations of 10 mg/L, to examine the effect of contact time on fluoride removal. In the experiments, the samples were collected 1, 2, 3, 6, 9, 12, and 24 hr after the reaction. The third batch experiments were conducted at fluoride concentrations of 10-1,000 mg/L, to examine the effect of initial fluoride concentrations on fluoride removal. The samples were collected for fluoride measurement 6 hr after the reaction. The fourth batch experiments were performed to examine the effect of the initial solution pH, which was adjusted to the desired value with 0.1 M NaOH and/or 0.1 M HCl. All experiments were performed in triplicate.

2.3. Data Analysis

All of the parameters of the models were estimated using MS Excel 2010, with the solver add-in function incorporated into the program. The model parameter values were determined by nonlinear regression. The determination coefficient (R^2), chi-square coefficient (χ^2), and sum of square error (SSE) were used to analyze the data, and confirm the fit to the model. The expressions of R^2, χ^2, and SSE are given below:

$$R^2 = \sum_{i=1}^{m} (y_c - \overline{y_e})_i^2 \quad (1)$$

$$x^2 \sum_{i=1}^{m} \left[\frac{(y_3 - y_c)^2}{y_c} \right]_i \quad (2)$$

$$SSE = \sum_{i=1}^{m} (y_e - y_c)_i^2 \quad (3)$$

where, y_c is the calculated adsorption capacity from the model, y_e is the measured adsorption capacity from the experiment, and $\overline{y_e}$ is the average of the measured adsorption capacity.

3. Results and Discussion

3.1. Characteristics of Quintinite Particles

The characteristics of quintinite particles are presented in Figs. 1 and 2. The TEM image (Fig. 1(a)) demonstrates that the particles

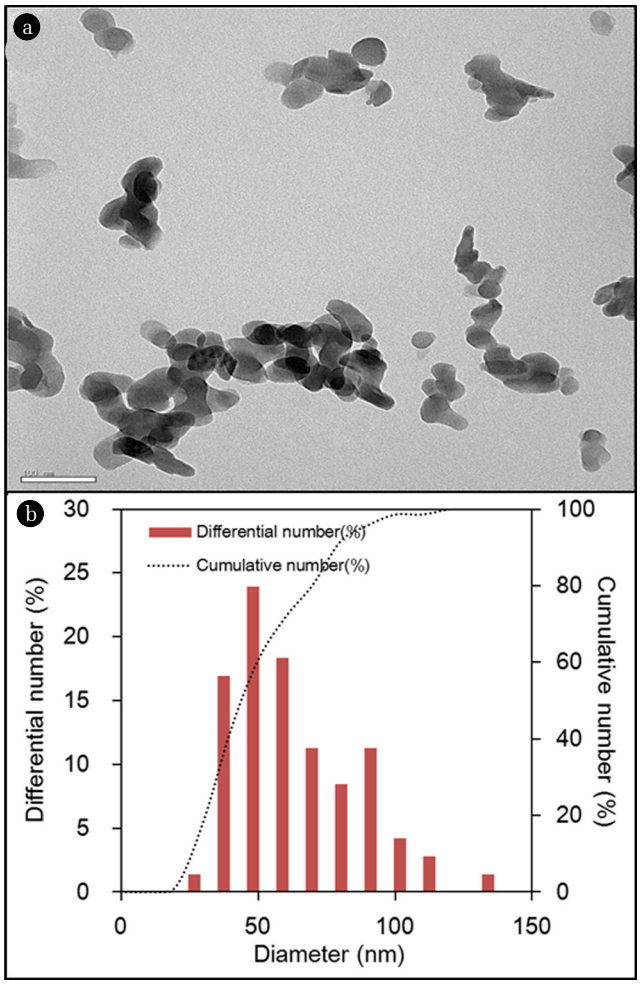

Fig. 1. Characteristics of quintinite particles: (a) transmission electron microscopy (TEM) image (bar=100 nm) and (b) particle size analysis based on the TEM image (number of particle=71).

were nano-sized. The particle size distribution (Fig. 1(b)) determined from the TEM image shows that the particle size was in the range from 20 to 120 nm, with a mean particle size of 59 nm. According to the XRD pattern (Fig. 2(a)), the particle had a layered structure, with sharp and intense lines at low 2θ, and less intense lines at high 2θ. The peaks observed at 2q=11.673, 23.469, 34.437, 35.978, 38.428, 41.652, 45.520, 60.675, and 62.025 (JCPDS 87-1138) correspond well with those of quintinite particles found in the literature [1]. The particle had a chemical formula of $Mg_4Al_2(OH)_{12}CO_3 \cdot 3H_2O$ with hexagonal crystal system (a=5.283 Å; c=15.159 Å). Based on the XRD pattern, the average crystal size (d) of the particle was estimated by the Debye-Scherrer formula [22]:

$$d = \frac{0.9\lambda}{\beta \cos\theta} \quad (4)$$

where, λ is the wavelength of the X-ray (=1.5406 Å), β is the full width at half maximum width of the diffraction peak (=0.369°), and θ is the diffraction angle (=11.673°/2). From the Debye-Scherrer analysis (inset in Fig. 2(a)), the value of d was calculated

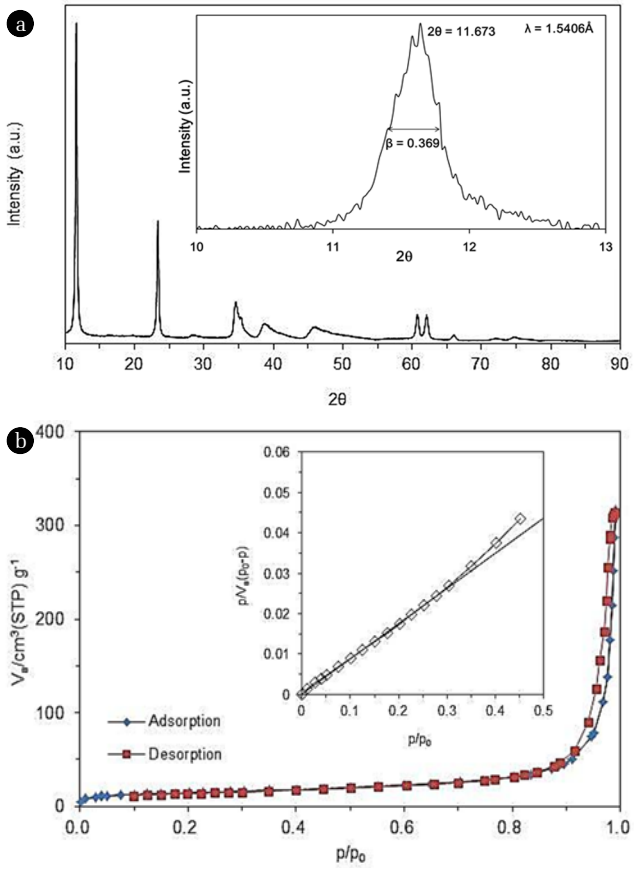

Fig. 2. Characteristics of quintinite particles: (a) X-ray diffraction pattern of quintinite particles (inset=Debye-Scherrer analysis) and (b) N_2 adsorption-desorption isotherms (inset=Brunauer-Emmett-Teller analysis).

to be 21.6 nm. Fig. 2(b) presents N_2 adsorption and desorption isotherms. According to the BET analysis (inset in Fig. 2(b)), the particles had a specific surface area of 49.8 m^2/g, and total pore volume of 0.4582 cm^3/g. From the BJH analysis, the mesopore volume was determined to be 0.4522 cm^3/g.

3.2. Characteristics of Fluoride Sorption to Quintinite Particles

Fig. 3(a) shows the effect of adsorbent dose on fluoride removal. The percent removal increased from 41.7%±0.3% to 89.8%±0.2% with increasing adsorbent doses from 0.1 to 2.0 g in 30 mL of solution. Meanwhile, the sorption capacity decreased from 1.26±0.01 to 0.14±0.01 mg/g with increasing adsorbent doses. Results indicate that the initial fluoride concentration of 10 mg/L could be reduced to <1.5 mg/L at the adsorbent dose ≥1.5 g. Fig. 3(b) provides the effect of reaction time on the removal of fluoride. The fluoride concentrations decreased rapidly with increasing reaction time, until the equilibrium was reached at 6 hr. The fluoride concentration dropped sharply to 2.7 mg/L (initial fluoride concentration=10 mg/L) at 1 hr of reaction time, and further decreased to 1.4 mg/L at 6 hr. Then, the fluoride concentration reached 1.2 mg/L at 24 hr of reaction time. Meanwhile, the sorption capacity increased from 0.15 to 0.18 mg/g, with increasing reaction time

from 1 to 24 hr.

Fig. 3(c) presents the effect of initial fluoride concentration on fluoride removal. At the lowest concentration of 10 mg/L, the percent removal was 87.6% and at the fluoride concentration of 100 mg/L, then decreased to 68.0%. At the highest concentration of 1,000 mg/L, the percent removal further decreased to 27.8%. Meanwhile, with increasing fluoride concentrations from 10 to 1,000 mg/L, the sorption capacity increased from 0.18 to 5.75 mg/g. Fig. 3(d) demonstrates the effect of initial solution pH on fluoride removal. The sorption capacity was 0.10 mg/g at pH 3, and increased to 0.17 mg/g at pH 5. The sorption capacity remained relatively constant at 0.17-0.18 mg/g, between pH 5 and pH 9. The sorption capacity dropped to 0.16 mg/g at pH 10, and then further decreased sharply to 0.09 mg/g.

Results demonstrate that the fluoride sorption in quintinite particles do not vary much at initial pH 4-10. This result could be related to the fact that during the sorption experiments, the final (equilibrium) pH converged to 8.1-8.8 (initial pH 4-10). Similar findings were reported in the literature by Kim et al. [14], showing that the fluoride sorption capacity of calcined Mg/Al LDH did not vary greatly between pH 4 and pH 9; the sorption capacity changed from 15.6 to 14.1 mgP/g, with increasing pH from 4 to 9. Han et al. [23] also reported that the removal of phosphate in the alginate beads containing calcined Mg/Al LDH was not sensitive to solution pH. They demonstrate that the percent removal of phosphate decreased slightly from 98.6% to 95.5%, as the solution pH increased from 4.9 to 8.9.

In our experiments, the fluoride sorption capacity considerably decreased at highly acidic (pH < 3) and alkaline pH (pH > 11) conditions. The fluoride sorption could decrease at highly acidic pH, due to the formation of hydrofluoric acid (HF), which is not favorable for adsorption onto the surfaces of adsorbent. According to MINTEQ calculation (Visual MINTEQ 3.0), HF species is formed at 35% of total F species (HF and F-) at pH 3. In addition, metal cations in quintinite might be dissolved at highly acidic pH, which results in the decrease of fluoride sorption [11]. At highly alkaline pH, the fluoride sorption could decrease, due to the competition between F- and OH- on the sorption sites. The contribution of NaF formation to the decrease of fluoride sorption might be negligible at highly alkaline pH. According to MINTEQ calculation, NaF species is only 0.2% of total F species (F- and NaF) at pH 11. Note that alkaline pH was obtained by adding 0.1 M NaOH in the experiments. Lv et al. [11] reported that phosphate removal in Mg/Al HTL decreased sharply from 110 to 5 mg/g, with increasing

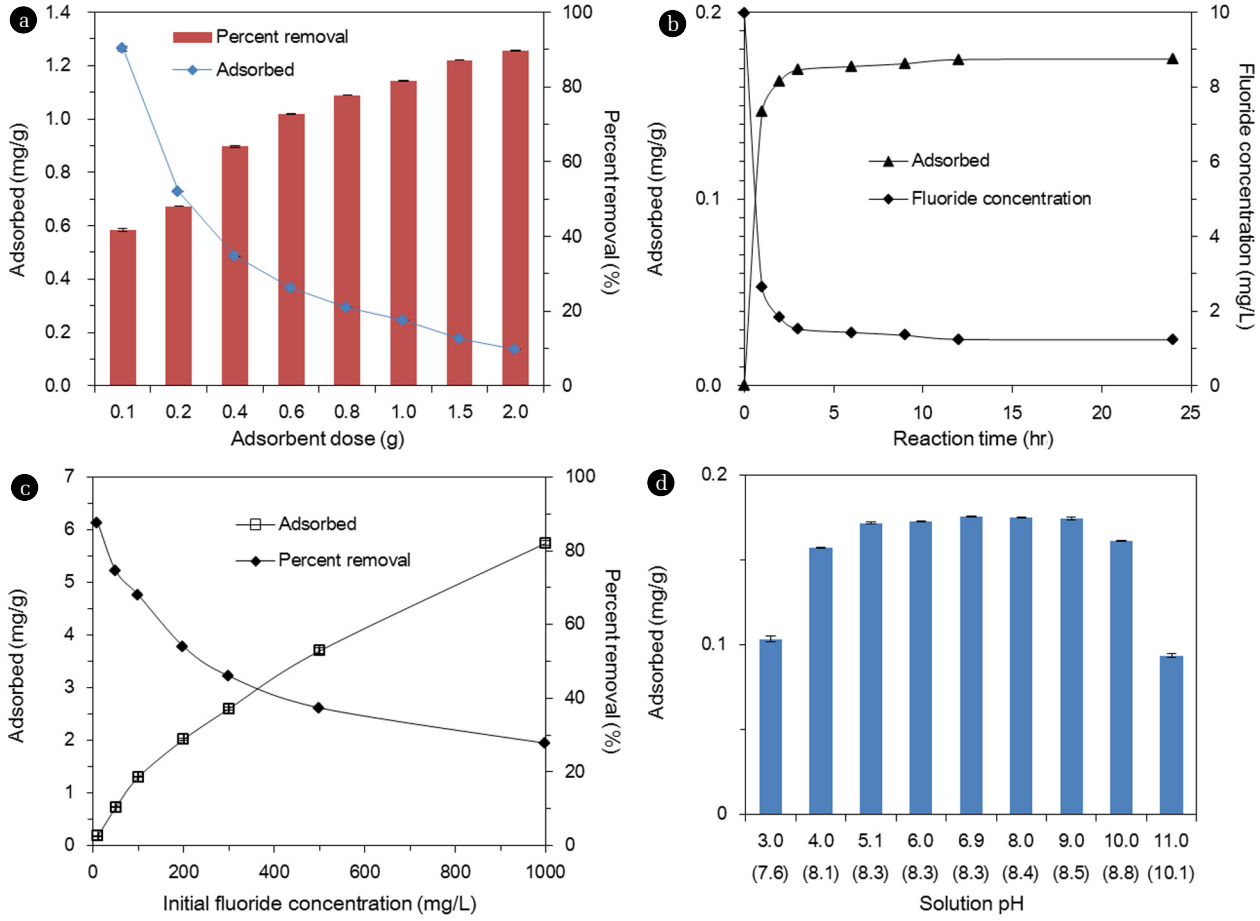

Fig. 3. Fluoride removal by quintinite particles: (a) effect of adsorbent dose, (b) effect of reaction time, (c) effect of initial fluoride concentration, and (d) effect of initial solution pH (the numbers in the parenthesis are final (equilibrium) pHs).

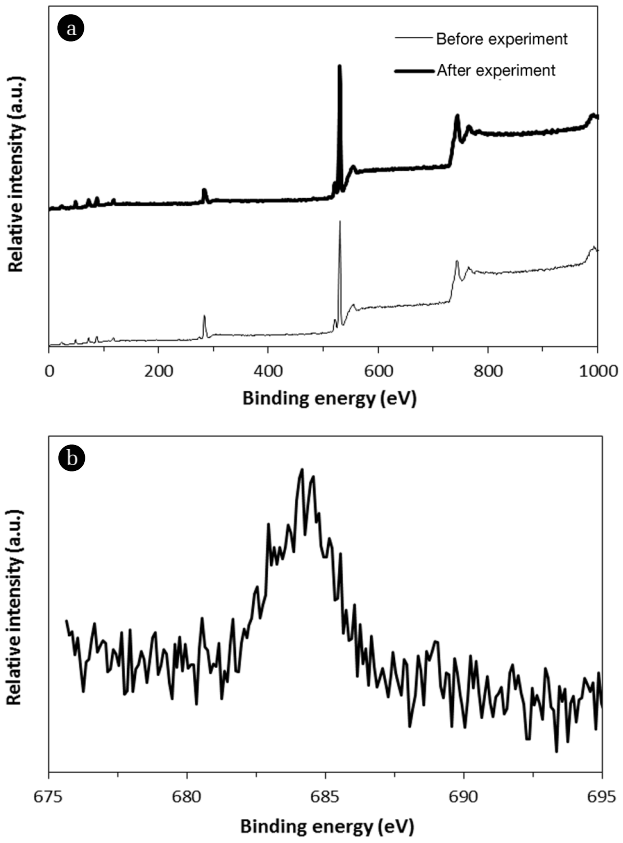

Fig. 4. X-ray photoelectron spectroscopy spectra: (a) wide scan before and after fluoride sorption experiments and (b) high-resolution scan of the F 1s region after fluoride sorption experiment.

pH from 5 to 10. Mandal and Mayadevi [21] showed that phosphate removal in Zn/Al HTL had an increasing tendency between pH 2.5 and pH 6.2, but a decreasing one between pH 6.2 and pH 9.8.

Fig. 4 presents XPS spectra. In the wide scan before and after fluoride sorption experiments (Fig. 4(a)), the peaks at binding energy of 49.15 and 73.20 eV are assigned to Mg 2p and Al 2p, respectively. In the high-resolution scan of the F 1s region after fluoride sorption experiment (Fig. 4(b)), the peak at 683.4 eV is ascribed to adsorbed fluoride ion on the surfaces of quintinite [20]. It is known that the two mechanisms of interlayer anion exchange and surface adsorption could contribute to the removal of fluoride by quintinite particles [5]. In the anion exchange process, the charge balancing anion (carbonate) in the interlayer region is replaced by fluoride ion. In surface adsorption, the negatively charged fluoride could adsorb to the positively charged brucite-like layer, via electrostatic interaction [5].

3.3. Kinetic and Equilibrium Model Analyses

The reaction time data (Fig. 3(b)) were analyzed, using the following nonlinear forms of pseudo-first-order (Eq. (5)), pseudo-second-order (Eq. (6)), and Elovich (Eq. (7)) kinetic models:

$$q_t = q_e(1-e^{-k_1 t}) \tag{5}$$

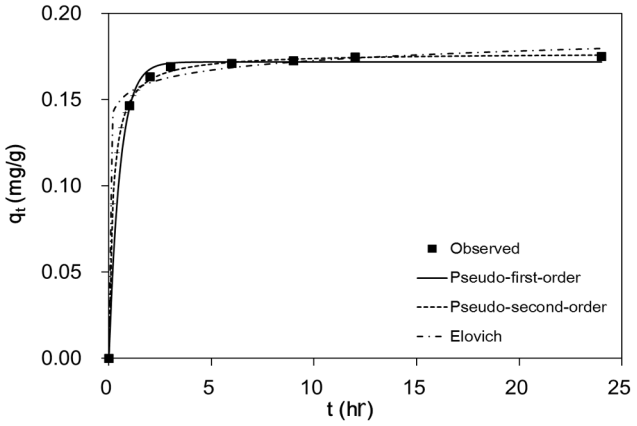

Fig. 5. Kinetic sorption model analysis. model parameters are provided in table 1.

$$q_t = \frac{k_2 q_e^2 t}{1+k_2 q_e t} \tag{6}$$

$$q_t = \frac{1}{\beta} ln(\alpha\beta) + \frac{1}{\beta} ln t \tag{7}$$

where, q_t is the amount of fluoride removed at time t, q_e is the amount of fluoride removed per unit mass of adsorbent at equilibrium, k_1 is the pseudo-first-order rate constant, k_2 is the pseudo-second-order velocity constant, α is the initial adsorption rate constant, and β is the Elovich adsorption constant.

The kinetic data and model fits for fluoride sorption to quintinite are shown in Fig. 5. Model parameters for the pseudo-first-order, pseudo-second-order, and Elovich models are provided in Table 1. In the pseudo-first-order model, the value of q_e was 0.17 mg/g, and the value of k_1 was 1.85 (1/hr). The value of q_e from the pseudo second-order model was similar to that from the pseudo-first-order model. The value of q_e was 0.18 mg/g, and the value of k_2 was 28.80 g/mg/hr. In the Elovich model, the values of α and β were 1.90E+06 mg/g/hr and 125.0 g/mg, respectively. The values of R^2, χ^2, and SSE indicate that the pseudo-second-order model was the most suitable for describing the data. This finding indicates that chemisorption is involved in the adsorption of fluoride to quintinite. In the literature, Cai et al. [7] reported that the kinetic data for fluoride sorption to calcined Mg/Al LDH were found to fit very well the pseudo-second-order model. Zhou et al. [20] also reported that the pseudo-second-order model was suitable for describing the adsorption kinetics of fluoride on calcined Li/Al LDH.

The fluoride concentration data (Fig. 3(c)) were analyzed using the following nonlinear forms of the Freundlich (Eq. (8)), Langmuir (Eq. (9)), and Redlich-Peterson (Eq. (10)) isotherm models:

$$q_e = K_F C_e^{1/n} \tag{8}$$

$$q_e = \frac{Q_m K_L C_e}{1+k_L C_e} \tag{9}$$

$$q_e = \frac{K_R C_e}{1+a_R C_e^g} \tag{10}$$

Table 1. Kinetic Model Parameters Obtained from Model Fitting to Experimental Data

Pseudo-first-order model					Pseudo-second-order model					Elovich model				
q_e (mg/g)	k_1 (1/hr)	R^2	χ^2	SSE	q_e (mg/g)	k_2 (g/mg/hr)	R^2	χ^2	SSE	α (mg/g/hr)	β (g/mg)	R^2	χ^2	SSE
0.17	1.85	0.92	2.75E−04	4.62E−05	0.18	28.80	0.98	9.19E−05	1.50E−05	1.90E+06	125.0	0.78	8.39E−03	1.36E−03

SSE: sum of square error.

Table 2. Equilibrium Model Parameters Obtained from Model Fitting to Experimental Data

Freundlich model						Langmuir model					Redlich-Peterson model						
K_F (L/g)	1/n	q_m (mg/g)	R^2	χ^2	SSE	Q_m (mg/g)	K_L (L/mg)	R^2	χ^2	SSE	K_R (L/g)	a_R (L/mg)	K_R/a_R (mg/g)	g	R^2	χ^2	SSE
0.20	0.51	6.78	1.00	0.028	0.027	7.71	0.0035	0.97	1.50	0.67	3.64	17.72	0.20	0.49	1.00	0.028	0.027

SSE: sum of square error.

where, C_e is the concentration of fluoride in the aqueous solution at equilibrium, K_F is the distribution coefficient, $1/n$ is the Freundlich constant, Q_m is the maximum mass of fluoride removed per unit mass of adsorbent (removal capacity), K_L is the Langmuir constant related to the binding energy, K_R is the Redlich-Peterson constant related to the adsorption capacity, a_R is the Redlich-Peterson constant related to the affinity of the binding sites, and g is the Redlich-Peterson constant related to the adsorption intensity.

Fig. 6 shows the equilibrium data and isotherm model fits for fluoride sorption to quintinite. Table 2 summarizes the equilibrium isotherm parameters for the Langmuir, Freundlich, and Redlich-Peterson models. The values of R^2, χ^2, and SSE indicate that both the Freundlich and Redlich-Peterson models were suitable for describing the data. Note that the Redlich-Peterson model fit was superimposed on the Freundlich fit (Fig. 6). The Redlich-Peterson model can be reduced to the Freundlich model, if K_R and a_R are much greater than unity [24]. In the Freundlich model, the value of K_F was 0.20 L/g, which corresponded well to the value of K_R/a_R in the Redlich-Peterson model. The value of $1/n$ was equivalent to the value (0.51) of (1–g). The adsorption capacity (q_m) was calculated from K_F and $1/n$, using the following equation [25]:

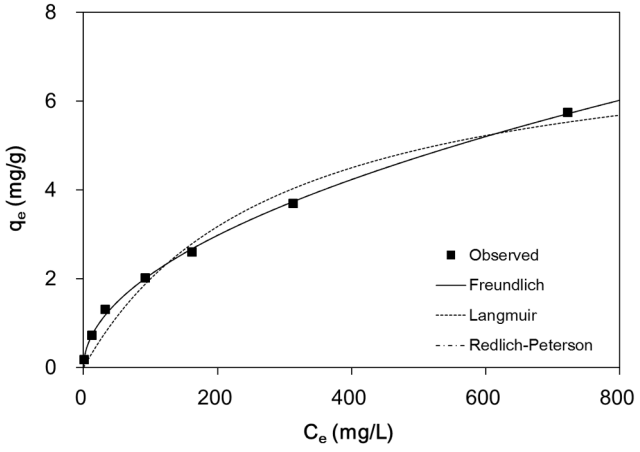

Fig. 6. Equilibrium isotherm model analysis. Model parameters are provided in table 2.

Table 3. Maximum Adsorption Capacity of Fluoride in HTL or MMO Particles Reported in the Literature (from the Langmuir isotherm analysis)

Adsorbent	Initial F conc. (mg/L)	Adsorption capacity (mg/g)	Reference
Quintinite	10-1,000	7.71	This study
Mg/Al MMO	5-50	36.86	[7]
Li/Al MMO	50-500	128.2-158.7	[21]
Mg/Al HTL	10-1,000	416.67	[13]
Mg/Al/Fe MMO	3-60	14.92	[11]
Zn/Al HTL	5.6-51.4	4.14	[14]
Mg/Al MMO	3.5-500	213.2	[16]
Mg/Al HTL	5-2,500	319.8a	[12]
Zn/Al MMO	2-60	13.4	[19]

HTL: hydrotalcite-like, MMO: mixed metal oxide.
[a] Maximum adsorption capacity obtained from the Langmuir-Freundlich isotherm

$$q_m = K_F C_0^{1/n} \quad (11)$$

The value of q_m was calculated to be 6.78 mg/g.

Table 3 summarizes the fluoride sorption capacities of hydrotalcite-like particles or mixed metal oxides from the literature. The maximum adsorption capacity (q_m) of quintinite in this study was determined to be 7.71 mg/g from the Langmuir model, which in Table 3 is in the low range of adsorption capacity. In order to improve the fluoride sorption capacity of quintinite, thermal treatment of quintinite at high temperatures (≥300°C) is recommended, which results in the increase of the BET surface area and fluoride sorption capacity [14]. Consequently, it is expected that the cost effectiveness of the adsorbent in fluoride removal can be improved.

4. Conclusions

In this study, the sorption of fluoride to quintinite was examined, using batch experiments. Results showed that the maximum adsorption capacity of fluoride to quintinite was 7.71 mg/g. The adsorption of fluoride to quintinite was not changed at pH 5-9, but decreased considerably in the highly acidic (pH < 3) and

alkaline (pH > 11) solution conditions. Kinetic model analysis showed that the pseudo second-order model was the most suitable for describing the kinetic data. Equilibrium isotherm model analysis demonstrated that both the Freundlich and Redlich-Peterson models were suitable for describing the equilibrium data. This study demonstrated that quintinite could be used as an adsorbent for the removal of fluoride from aqueous solutions.

Acknowledgments

This work was supported by the National Research Foundation of Korea, funded by the Ministry of Education, Republic of Korea (No. 2014-027899).

References

1. Delorme F, Seron A, Gautier A, Crouzet C. Comparison of the fluoride, arsenate and nitrate anions water depollution potential of a calcined quintinite, a layered double hydroxide compound. *J. Mater. Sci.* 2007;42:5799-5804.
2. Miyata S. Anion-exchange properties of hydrotalcite-like compounds. *Clays Clay Miner.* 1983;31:305-311.
3. Hernandez-Moreno MJ, Ulibarri MA, Rendon JL, Serna CJ. IR characteristics of hydrotalcite-like compounds. *Phys. Chem. Miner.* 1985;12:34-38.
4. Costantino U, Marmottini F, Nocchetti M, Vivani R. New synthetic routes to hydrotalcite-like compounds: characterisation and properties of the obtained materials. *Eur. J. Inorg. Chem.* 1998;1998:1439-1446.
5. Goh KH, Lim TT, Dong Z. Application of layered double hydroxides for removal of oxyanions: a review. *Water Res.* 2008;42:1343-1368.
6. Ma W, Zhao N, Yang G, Tian L, Wang R. Removal of fluoride ions from aqueous solution by the calcination product of Mg-Al-Fe hydrotalcite-like compound. *Desalination* 2011;268:20-26.
7. Cai P, Zheng H, Wang C, et al. Competitive adsorption characteristics of fluoride and phosphate on calcined Mg-Al-CO3 layered double hydroxides. *J. Hazard. Mater.* 2012;213-214:100-8.
8. Ayoob S, Gupta AK. Fluoride in drinking water: a review on the status and stress effects. *Crit. Rev. Environ. Sci. Technol.* 2006;36:433-487.
9. Mohapatra M, Anand S, Mishra BK, Giles DE, Singh P. Review of fluoride removal from drinking water. *J. Environ. Manag.* 2009;91:67-77.
10. Bhatnagar A, Kumar E, Sillanpää M. Fluoride removal from water by adsorption: a review. *Chem. Eng. J.* 2011;171:811-840.
11. Lv L, He J, Wei M, Evans DG, Zhou Z. Treatment of high fluoride concentration water by MgAl-CO3 layered double hydroxides: kinetic and equilibrium studies. *Water Res.* 2007;41:1534-1542.
12. Batistella L, Venquiaruto LD, Luccio MD, et al. Evaluation of acid activation under the adsorption capacity of double layered hydroxides of Mg-Al-CO3 type for fluoride removal from aqueous medium. *Ind. Eng. Chem. Res.* 2011;50:6871-6876.
13. Mandal S, Mayadevi S. Defluoridation of water using as-synthesized Zn/Al/Cl anionic clay adsorbent: Equilibrium and regeneration studies. *J. Hazard. Mater.* 2009;167:873-878.
14. Kim JH, Lee CG, Park JA, Kang JK, Yoon SY, Kim SB. Fluoride removal using calcined Mg/Al layered double hydroxides at high fluoride concentrations. *Water Sci. Technol. Water Supply* 2013;13:249-256.
15. Lv L. Defluoridation of drinking water by calcined MgAl-CO3 layered double hydroxides. *Desalination* 2007;208:125-133.
16. Wang H, Chen J, Cai Y, Ji J, Liu L, Teng HH. Defluoridation of drinking water by Mg/Al hydrotalcite-like compounds and their calcined products. *Appl. Clay Sci.* 2007;35:59-66.
17. Lv L, He J, Wei M, Evans DG, Duan X. Factors influencing the removal of fluoride from aqueous solution by calcined Mg-Al-CO3 layered double hydroxides. *J. Hazard. Mater.* 2006;133:119-128.
18. Das DP, Das J, Parida K. Physicochemical characterization and adsorption behavior of calcined Zn/Al hydrotalcite-like compounds (HTlc) towards removal of fluoride from aqueous solution. *J. Colloid Interface Sci.* 2003;261:213-220.
19. Díaz-Nava C, Solache-Ríos M, Olguín MT. Sorption of fluoride ions from aqueous solutions and well drinking water by thermally treated hydrotalcite. *Sep. Sci. Technol.* 2003;38:131-147.
20. Zhou J. Cheng Y. Yu J. Liu G. Hierarchically porous calcined lithium/aluminum layered double hydroxides: facile synthesis and enhanced adsorption towards fluoride in water. *J. Mater. Chem.* 2011;21:19353-19361.
21. Mandal S, Mayadevi S. Adsorption of fluoride ions by Zn-Al layered double hydroxides. *Appl. Clay Sci.* 2008;40:54-62.
22. Yu CH, Al-Saadi A, Shih SJ, Qiu L, Tam KY, Tsang SC. Immobilization of BSA on silica-coated magnetic iron oxide nanoparticle. *J. Phys. Chem. C* 2009;113:537-543.
23. Han YU, Lee WS, Lee CG, Park SJ, Kim KW, Kim SB. Entrapment of Mg-Al layered double hydroxide in calcium alginate beads for phosphate removal from aqueous solution. *Desalination Water Treat.* 2011;36:178-186.
24. Zhang L, Hong S, He J, Gan F, Ho YS. Adsorption characteristic studies of phosphorus onto laterite. *Desalination Water Treat.* 2011;25:98-105.
25. Halsey G. Physical adsorption on non-uniform surfaces. *J. Chem. Phys.* 1948;16:931-937.